Mon. Not. R. Astron. Soc. **319**, 677–684 (2000)

Behaviour of radiative accelerations in stars

G. Alecian[1]★ and F. LeBlanc[2]★

[1]*Laboratoire d'Astrophysique Extragalactique et de Cosmologie, CNRS-(UMR 8631), Observatoire de Paris, Université Paris 7. DAEC, Observatoire de Meudon, F-92195 Meudon Cedex, France*

[2]*Département de physique et d'astronomie, Université de Moncton, Moncton, N.-B., E1A 3E9, Canada*

Accepted 2000 March 22. Received 2000 March 20; in original form 1999 November 8

ABSTRACT

Diffusion processes are able to stratify elements in stars on time-scales shorter than the evolution time on the main sequence. According to the efficiency of these diffusion processes, which depend on the radiative accelerations, abundances are time-dependent and inhomogeneous outside the stellar core. Large atomic and opacity data bases allow accurate computations of radiative accelerations, and several authors have developed efficient methods taking advantage of these large data bases. In the present work, these powerful tools are used to improve our knowledge on how radiative accelerations depend on the abundances of elements in stellar plasma.

In this study, we test the behaviours of radiative accelerations that are usually supposed. The results we obtain give some clues for future attempts to simplify the calculations of these accelerations.

Key words: diffusion – stars: abundances.

1 INTRODUCTION

The knowledge of radiative accelerations is important in several problems related to the modelling of stars. Radiative acceleration is often the leading component in diffusion processes which can produce abundance significant stratifications of elements in stars. The consequences of such stratifications are clearly important for stars as chemically peculiar A and F stars, but it appears now that they could also affect the properties of normal stars (Turcotte et al. 1998a; Turcotte et al. 1998b).

Since the beginning of the 1990s, the availability of large atomic and opacity data bases (Rogers & Iglesias 1992a,b; Seaton et al. 1992) allows accurate computations of radiative accelerations. Several authors (Gonzalez et al. 1995b, hereafter referred to as GLAM; Seaton 1997, hereafter referred to as S97) have developed new methods which take advantages of these large data bases. Recently, studies using these methods have been undertaken for stellar envelopes (Turcotte et al. 1998a, 1998b; Richer et al. 2000), and many interesting results show the extensive possibilities of such studies for future modelling of stars.

The methods for computing radiative accelerations from the studies previously mentioned (GLAM, S97) are, of course, very valuable for accurate quantitative calculation of diffusion, but each of them has specific drawbacks. Both methods of the Canadian group (GLAM and sampling methods) are very CPU-time consuming, they need large numerical codes to produce radiative accelerations, and are very heavy to handle. The method developed by Seaton, which uses interpolations in tables produced by a sampling method (close to the one previously mentioned) is fast and accurate. These tables are available at the CDS (Centre de Données astronomiques de Strasbourg). However, this method is closely dependent on the tables that M. J. Seaton made available: the user cannot update them in case of new atomic data (these tables are restricted to ions available in Opacity Project data, Seaton et al. 1992) or in case of some other specific needs. For instance, it can be sometimes necessary to compute the accelerations for abundances outside the limits allowed by the tables of S97. The sampling method can also become inaccurate for small abundances of the element under consideration and at low temperatures, when absorption lines are too narrow with respect to the frequency mesh of the opacity tables.

Apart from quantitative studies of diffusion, these methods can also be used to understand the behaviour of radiative accelerations with respect to the local properties of the medium (such as local abundances). This is very interesting, because it is now possible from these accurate methods, to check the validity of other methods, perhaps less accurate, but in principle much easier to use and, to some extent, more general. Such a method has already been developed by Alecian & Artru (1990) who have established an approximate formula for the radiative accelerations. However, their method is only valid for elements which have abundances that are small enough not to affect the local plasma conditions (commonly called the test particle approximation), and assumes that absorption lines which contribute to the accelerations have Lorentz profiles. Contribution of photoionization is neglected. As a result of this, this method cannot apply to elements such as Fe or CNO which can be dominant in opacities (even at solar abundances) and for which absorption through photoionization cannot be neglected. This approximate method was based on a poor knowledge of the behaviour of radiative accelerations with

★ E-mail: georges.alecian@obspm.fr (GA); leblanfn@umonton.ca (FL)

respect to local plasma conditions. The purpose of the present work is to improve this knowledge in view of further attempts.

In Section 2, we formalize the classical knowledge about radiative acceleration; in Section 3 to compute radiative acceleration, we discuss the details of the methods we have used in the computations presented in Section 4 in stars. Section 5 is a general discussion.

2 APPROXIMATE FEATURES

The radiative acceleration through a single line l (we first consider only bound–bound transitions) of an ion A^{+i} (with number density n_i) can be expressed as

$$g_{il} = (n_{ik}/A_i m_p c n_i) \int_0^\infty \sigma_{i,km} \phi_\nu \mathrm{d}\nu, \quad (1)$$

where ϕ_ν is the photon energy flux ($\mathrm{erg\,cm^{-2}\,s^{-1}}$) between frequency ν and $\nu + \mathrm{d}\nu$, $\sigma_{i,km}$ the absorption cross-section from level k to m corresponding to the line l, and n_{ik} the number of ions A^{+i} in level k. A_i, m_p and c are, respectively, the atomic mass of the ion, the proton mass and the velocity of light.

Since Michaud (1970), radiative accelerations (g_{rad}) have been very often discussed and computed (see for instance Michaud et al. 1976; Alecian & Michaud 1981; GLAM, S97). When redistribution among ions is neglected and when only an average radiative acceleration is required for the element under consideration, radiative accelerations can be expressed in a way that does not consider individual atomic transitions, and which is well fitted for the use of large and detailed opacity tables (see equation 1 of Richer et al. 1998).

In the present work we are mainly interested in how g_{rad} depends on the local concentration of A^{+i}, because this dependency is at the origin of the main non-linearity in the process of abundance stratification in stars (see Alecian & Grappin 1984). A first approach consists in noting that the photon flux ϕ_ν, in the diffusion approximation, is inversely proportional to the local monochromatic opacity. This opacity can be expressed as the sum of two quantities: $\kappa_{il} + \kappa_{\mathrm{tot\ b}}$, where κ_{il} is the opacity owing the line l of A^{+i} and $\kappa_{\mathrm{tot\ b}}$ a 'total background' monochromatic opacity owing to all other sources of opacity, including the other transitions of the ion A^{+i}. Noting that $\kappa_{il} = n_{ik}\sigma_{i,km}$ (in $\mathrm{cm^{-1}}$), equation (1) can be written as

$$g_{il} = (\kappa_R/n_i) \int_0^\infty [\kappa_{il}/(\kappa_{il} + \kappa_{\mathrm{totb}})] f \mathrm{d}\nu, \quad (2)$$

where κ_R is the Rosseland average and f is a function independent of n_i. The integral is close to zero outside a frequency range of several times the line width around ν_l, the central frequency of line l.

If we consider that the test-particle approximation is valid, and that there is no significant line overlapping, κ_R and $\kappa_{\mathrm{tot\ b}}$ can be considered as independent of n_i in equation (2). Schematically, the integral in equation (2) has two asymptotic cases (see for instance Alecian & Vauclair 1983): (i) the weak line case where $\kappa_{il} \ll \kappa_{\mathrm{tot\ b}}$ for $\nu = \nu_l$, and (ii) the strong line (or saturated) case where $\kappa_{il} \gg \kappa_{\mathrm{tot\ b}}$ for $\nu = \nu_l$. This latter case leads to define a saturation threshold χ_S, which corresponds to the element abundance (with respect to the Sun, according to the same definition as S97) such as for $\chi = \chi_S$ one has $\kappa_{il} = \kappa_{\mathrm{tot\ b}}$. In the first case (i), g_{il} is independent of n_i since the ratio n_{ik}/n_i (see equation 1) is fixed by the Boltzmann law. In the second case (ii), g_{il} depends on n_i according to the line profile: $g_{il} \propto n_i^{-1/2}$ for Lorentz profile, and approximately $g_{il} \propto n_i^{-1}$ for Gauss profile. This behaviour can be summarized by saying that the slope of the function g_{il} with respect to n_i, is 0 in case (i), and between -0.5 and -1 in case (ii) of a Voigt profile.

The total radiative acceleration on ion A^{+i} is given by adding all contributions of bound–bound transitions and also the contribution of bound–free transitions $g_{i,\mathrm{cont}}$ (see discussion in Alecian 1994; Massacrier 1996):

$$g_i = \Sigma_l g_{il} + g_{i,\mathrm{cont}}. \quad (3)$$

Generally, $g_{i,\mathrm{cont}}$ is significantly smaller than the total contribution of bound–bound transitions, however, it cannot always be neglected, especially in case of light elements, low ionization degrees or when the saturation effect of bound–bound transitions is strong (Alecian 1994). One can suppose that $g_{i,\mathrm{cont}}$ does not depend on the local concentration of the element. However, this is not always justified, in particular when that term is important in equation (3).

Therefore, according to the above discussion and to the approximation proposed by Alecian (1985), the radiative acceleration can be approximately described by the following normalized function

$$\gamma_{\mathrm{rad}} = (1 + X)^\alpha + \gamma_{\mathrm{cont}}. \quad (4)$$

The exponent α is $-1.0 < \alpha < -0.5$, and X is the normalized concentration $X = \chi/\chi_S$. The acceleration owing to photoionization γ_{cont} is assumed constant (generally much smaller than 1). One has $\gamma_{\mathrm{rad}} \approx 1$ when the element concentration (X) tends to zero. Figs 1(a) and (b) show γ_{rad} and its derivative with respect to X, assuming arbitrarily $\gamma_{\mathrm{cont}} = 10^{-3}$. One can note in Fig. 1 that the acceleration is almost constant for a small relative concentration of the ion ('unsaturated' case, left part of Fig. 1b), it is decreasing with a slope close to α when saturation occurs ('saturated' case, centre part of Fig. 1b), and it tends to γ_{cont} for strong concentrations ('oversaturated' case, right part of Fig. 1b). The derivative gives very interesting information about the dominant physical processes at work for radiative accelerations: the decrease points out the beginning of the saturation effect, and the increase shows for which abundance the acceleration owing to photoionization dominates bound–bound transitions. Moreover, the minimum value of the derivative depends strongly on the line profile.

This is the classical knowledge about the behaviour of radiative accelerations. It is mainly based on the following approximations: (i) effects of blends are negligible; (ii) the Rosseland opacity is supposed to be independent of the ion concentration; (iii) all the lines of the ion saturate for the same concentration; (iv) all the lines have the same profile; (v) the radiative acceleration owing to photoionization is supposed to be small and independent of the ion concentration. Detailed computations (with GLAM or sampling methods for instance) do not have these limitations and are supposed to be accurate to better than 30 per cent. However, the real importance of these approximations and equation (4) have never been closely verified and this is one of the purposes of the present work.

3 METHODS TO COMPUTE RADIATIVE ACCELERATIONS

3.1 The GLAM and the sampling methods

The GLAM method employs averaged monochromatic values for

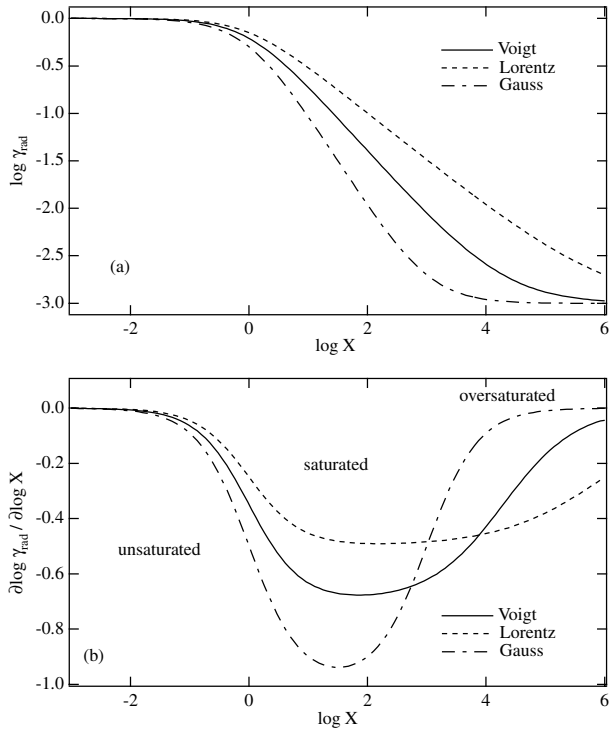

Figure 1. Schematic behaviour of the normalized radiative acceleration with respect to the relative concentration of the considered ion (see text). The dashed line is for Lorentz profile ($\alpha = -0.5$), the point–dashed line is the approximation for the Gauss profile ($\alpha = -1$), and the continuous line mimics the case of a Voigt profile ($\alpha = -0.7$). Panel (a) shows the radiative acceleration. Panel (b) shows the logarithmic derivative of the acceleration. The minimum value is close to the exponent α. The increase of the slope depends on the value assumed for γ_{cont}, here it is set to $\gamma_{cont} = 10^{-3}$.

the background opacity $\kappa_{tot\ b}$ (see GLAM for more details). This average opacity is calculated in 4000 evenly spaced intervals in $u = h\nu/kT$ between $0 < u \leq 20$. This calculation is performed once, for each element considered, on a temperature–electronic-density grid and these tables are then used in radiative acceleration calculations (see section 3 of GLAM for more details). Equation (2) is integrated for each individual bound–bound or bound–free transition. For bound–bound transitions, the background opacity used, which is the total average opacity minus the contribution of the transition in question, is the one associated with the Δu interval in which the natural frequency of the line is found. Thus the background opacity is considered to be a constant in each line. Equation (2) is also integrated for each individual bound–free transition, but since these transitions can span several Δu intervals, $\kappa_{tot\ b}$ is varied appropriately during these calculations. This method has been used to calculate the radiative accelerations of CNO (Gonzalez et al. 1995a), Fe (LeBlanc & Michaud 1995) and Ne, Mg, Si, S and Ar (LeBlanc, Michaud & Richer 2000; hereafter referred to as LMR2000). In all these studies the OP atomic data were used except for Fe I and Fe II for which the Kurucz (1990, 1991) data were employed. Since each transition is treated individually, the GLAM method has the advantage that it can take into account the redistribution of momentum among the ions (see section 5 of GLAM for more details).

Tables of radiative accelerations are constructed on the same temperature–electronic-density grid as mentioned above for each element considered. Tables are calculated for several values of the abundance of the element considered while the abundances of the other atomic species are kept at their relative solar values. To obtain the radiative accelerations in a given stellar model an interpolation method is used. The use of these tables has the disadvantage that it renders the inclusion of the effect of the diffusion of the other elements on the radiative force of the element considered (i.e. blending effects) impossible. The GLAM calculations presented here include the elements H, He, C, N, O, Ne, Mg, Si, S, Ar, Ca and Fe. Details concerning such calculations can be found in LMR2000 and in GLAM.

Another method that can be employed to calculate radiative accelerations is the sampling method, in which the opacity of the elements is calculated at a certain number of frequency points (typically 10^4 to 10^5 points). These monochromatic opacities are then used in the integration of equation (2). For numerical efficiency an opacity spectrum for each element is calculated at each temperature–electronic-density point desired and thus redistribution of momentum among the ions cannot be directly included. The monochromatic opacities of the elements considered have to be sampled at a large number of frequency points especially in the outer regions of stars where the atomic lines are narrow (see LMR2000 for more details). The opacity sampling method is well suited to study the blending effects but is numerically onerous.

3.2 The Seaton method

S97 has used the sampling method to compute the radiative accelerations for all the ions for which the atomic data are available in TOPbase (Cunto et al. 1993). He has also built a set of tables with a mesh of values of temperature and electron density which allows recalculation of the accelerations by interpolation for any abundance (χ) with respect to the solar values in the interval $-2 \leq \log \chi \leq 4$ (according to S97). These tables and the interpolation codes are available at CDS.

We have used these tables and interpolation codes to compute the detailed and extensive accelerations presented in Section 4. Some parts of the original codes at the CDS have been modified by us and by G. Legris (1998)) to adapt them to our purpose (see Section 4 for more details).

3.3 Comparison of the Seaton versus the GLAM methods

Owing to the method used to evaluate the background opacity in the GLAM method, it generally underestimates the g_{rad} value for temperatures up to approximately 10^6 K (LMR2000). Since the line opacity is evenly distributed in the frequency interval in which its natural frequency is found, at low temperatures the valleys in the opacity spectrum are artificially erased since the line widths are narrower than the Δu intervals used. This induces a decrease of the flux peaks and thus decreases g_{rad}. At high temperatures the line widths become wider than the frequency intervals and the GLAM method slightly overestimates g_{rad}. The GLAM method inherently underestimates the g_{rad} as compared with the sampling method through most of the structure of the stars.

Beside the differences owing to the treatment of the background opacity between the GLAM and the Seaton method, other factors also contribute to the differences observed between their respective g_{rad} results: S97 includes fine structure in his calculations while GLAM does not, there are also more elements included in

S97 than in GLAM. Thus the radiative accelerations given by the Seaton codes and tables are generally larger than those given by the GLAM method (see LMR2000).

3.4 The parametric approximation versus the Seaton method

A semianalytic approximation (often called parametric approximation) has been developed by Alecian (1985) and Alecian & Artru (1990). It consists in using a simplified form of the radiative acceleration obtained by separating the atomic quantities from those describing the local plasma. The same approximations as for equation (4) are assumed. Roughly, in this simplified form, the acceleration depends on two quantities (Φ and Ψ) gathering the atomic properties of the considered ion and depending weakly on temperature and electronic density. They are computed from detailed atomic data: (i) Φ depends mainly on the oscillator strength of the bound–bound transitions (ii) Ψ depends on their profile. The former gives the effect of the lines strength, the latter gives the saturation effect. Φ and Ψ do not depend on the concentration of the considered element, therefore they need not be recomputed when the local abundance changes. This is their most interesting property because, in diffusion processes calculations, concentration depends on time.

This approximate method has been used (in the case of iron) by Alecian et al. (1993) who have defined four levels of approximation. 'Approx.1' (the more accurate one) consists in computing Φ and Ψ at each layer of the star, 'Approx.2' consists in using constant values (different for each ion) for Φ and Ψ, 'Approx.2 adjusted' is the same as the previous one except that Φ and Ψ are calibrated from accurate and detailed computations, 'Approx.3' is the same as 'Approx.2' except that Φ and Ψ are obtained by extrapolation along the isoelectronic sequences. The latter method is only used when atomic data are missing.

We have made a comparison between accelerations obtained with these parametric approximations and those obtained with the Seaton method in the case of Ca, because this element has already been considered by S97 for the same purpose. We have made computations in a main-sequence star with $T_{\rm eff} = 8500$ K, log $g = 4.311$ (model communicated by J. Richer, see Richer & Michaud 1993). Our results are shown in Fig. 2**.** The quantities Φ and Ψ have been determined for Ca from TOPbase data available in 1999 May. Both parametric methods ('Approx.1' and 'Approx.2') are rather in a good agreement with the result obtained using the Seaton codes and tables. The agreement is clearly better than the one shown in fig. 16 of S97, which was computed for the same effective temperature but at a slightly different gravity (log $g = 4.26$). One can note that the main difference between our results and those of fig. 16 of S97 is that the accelerations obtained here using the Seaton codes and tables are much larger than those of S97. Nevertheless, these larger accelerations have been confirmed by M. Seaton (private communication) who computed for us the Ca acceleration using our stellar model and his own codes. The reason why he obtained lower accelerations for Ca in his previous work (S97) and then why the agreement with the parametric methods is better in our computations, are not understood and cannot be further investigated since the original data of S97 have been deleted (M. Seaton, private communication).

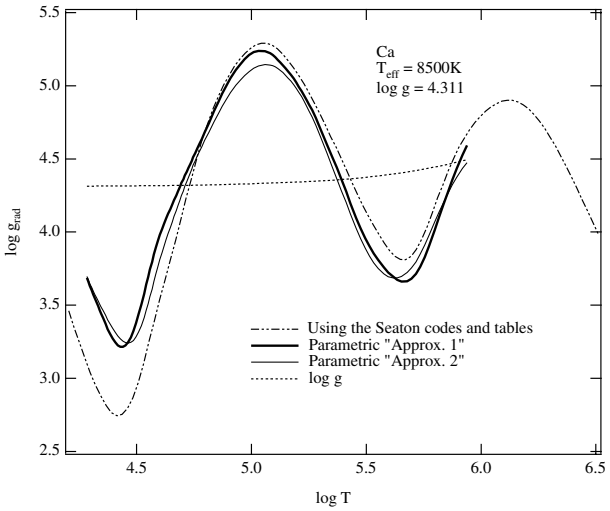

Figure 2. Radiative accelerations using the parametric approximation versus the one obtained using the Seaton codes and tables in the case of Ca. The curve 'log g' corresponds to the local gravity.

The accurate radiative accelerations obtained for Ca using the parametric method presented above cannot be generalized to other elements without detailed verification. It should also be noted that the parametric method cannot be used to study the behaviour of radiative accelerations since it is based on numerous approximations, presented in Section 2, which already imply several assumptions on that behaviour. However, we have used this method to estimate the saturation thresholds $\chi_{\rm S}$ (see next section). An improvement of the parametric method is planned in the near future.

4 COMPUTATIONS IN STARS

The main purpose of the present work is to study the behaviour of the radiative accelerations with respect to concentration of the elements and to compare this behaviour to the schematic one shown in Fig. 1. It is therefore important to consider only ions for which the saturation threshold is such that $-2 \leq \log \chi_{\rm S} \leq 4$, which corresponds to the maximum interval allowed for the use of Seaton's data. A priori, log $\chi_{\rm S}$ is unknown, it depends on the atomic properties of each ion and on the stellar model. The parametric method gives a convenient way to estimate this threshold (equation 3 of Alecian & Artru 1990)[1] for layers where ions are supposed to give their largest contribution to the total $g_{\rm rad}$. We have applied this method for the whole atomic data set available in TOPbase to find the ions such that $-2.0 \leq \log \chi_{\rm S}$. We have found only 20 ions that fulfil this condition, they are listed in Table 1. The column 'log $\chi_{\rm max}$' points out the abundance above which the element exceeds 10 per cent of mass fraction in the medium. We consider that for higher abundances, the physical meaning of our computations are very doubtful since our stellar model (see below) has been computed for solar metallicity. Note that log $\chi_{\rm max}$ is the same for all ions of a given element, while log $\chi_{\rm S}$ is different for each ion. One can notice that, even for the ions shown in Table 1, log $\chi_{\rm S}$ are small and this implies that 'unsaturated case' accelerations will be met with difficulty.

We have made computations (using the Seaton codes and tables) for all these ions in a main-sequence star with $T_{\rm eff} = 10\,000$ K, log $g = 4.31$ (model communicated by J. Richer, see Richer & Michaud 1993). This is a typical A type star where diffusion processes are important. We have built grids in χ of the radiative accelerations of individual ions and we have computed

[1] The equation (3) of Alecian & Artru (1990) must be corrected by dividing the right hand side by the mass-fraction of hydrogen.

Table 1. Ions with log χ_S larger than −2.0 in the layers where they give their maximum contribution to g_{rad}.

Ion	log χ_S	log χ_{max}
Na XI	−1.86	3.4
Ar XIII	−1.79	3.0
Ar XIV	−1.72	3.0
Ar XV	−1.69	3.0
Ar XVI	−1.88	3.0
Ca VIII	−1.96	3.2
Ca IX	−1.94	3.2
Ca XIII	−1.64	3.2
Ca XIV	−1.22	3.2
Ca XV	−0.97	3.2
Ca XVI	−0.87	3.2
Ca XVII	−0.87	3.2
Ca XVIII	−1.00	3.2
Fe XI	−1.93	1.9
Fe XII	−1.74	1.9
Fe XIII	−1.70	1.9
Fe XIV	−1.64	1.9
Fe XX	−1.62	1.9
Fe XXI	−1.45	1.9
Fe XXII	−1.64	1.9

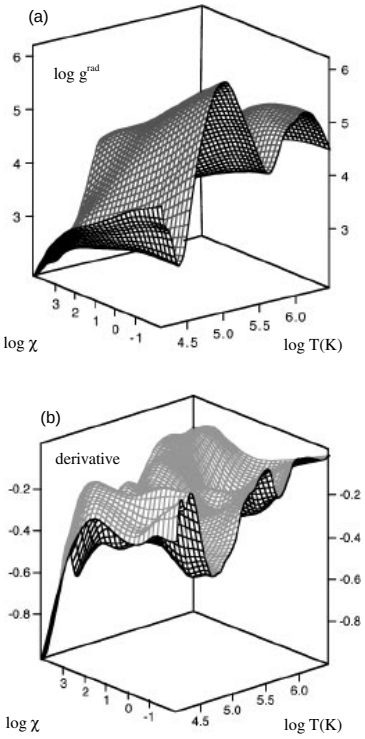

Figure 3. 3D graphs of the total acceleration and its logarithmic derivative of Ca versus the abundance (with respect to solar values) and versus the stellar depth (temperature). Panel (a) shows the radiative acceleration. Panel (b) shows the logarithmic derivative of the acceleration.

their derivative $\partial\log(g_i)/\partial\log(\chi)$. For these computations, we have adapted the routines M. Seaton made available at the CDS. To obtain the accelerations of individual ions we have changed the default weighting $W=1$ (for all ions) by setting $W=0$ for all ions except for the ion of interest, this part of the work had been started by G. Legris (1998). The derivatives which are not provided by S97, are computed with a classical centred five points formula (uncentred three points formula at the boundaries).

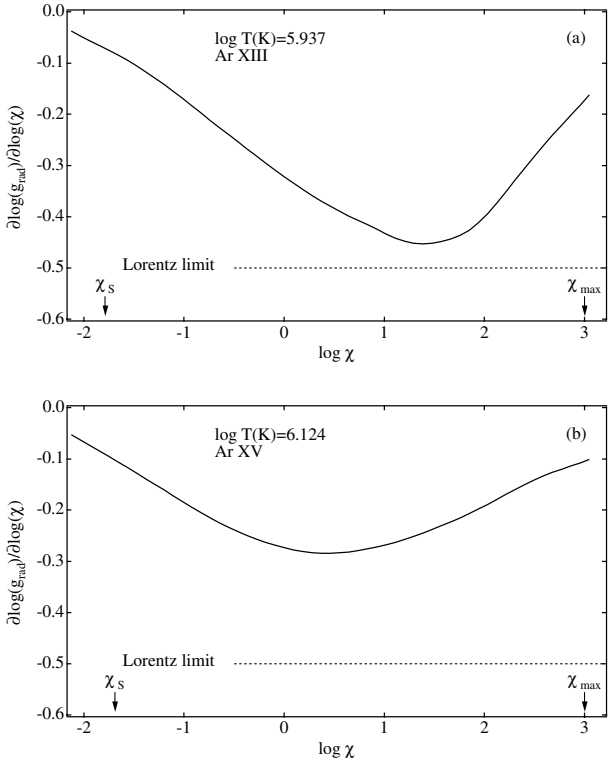

Figure 4. The logarithmic derivative of the acceleration with respect to the abundance for (a) Ar XIII and (b) Ar XV in a star with $T_{eff} = 10\,000$ K. For each ion, the computations have been carried out for the layer corresponding to the maximum population. The dashed line ('Lorentz limit') is the limit which should be reached by g_{rad} owing to bound–bound transitions in the case of pure Lorentz profile. The two arrows (χ_S and χ_{max}) correspond to the values given in Table 1.

Fig. 3 shows two 3D graphs of the total acceleration of Ca (sum of g_i over all ionization stages) and its logarithmic derivative, versus the abundance (with respect to solar values) and versus the stellar depth (temperature). This figure is an example of the grids of data we have built for each ion of each element. From these grids we can extract slices for any temperature or abundance.

To compare the real behaviour of g_{rad} (from these detailed computations) to the approximate one discussed in Section 2, we have plotted in Figs 4, 5 and 6 the logarithmic derivative of the accelerations, for individual ions, with respect to the abundance. For the sake of conciseness only six typical cases (Ar XIII, Ar XV, Ca XIV, Ca XVI, Fe XI and Fe XIII) are presented for this study. The derivatives have been computed as already mentioned (corresponding to a slice in grids of data like the one shown in Fig. 3b). The results presented here have been extracted for temperatures where each ion has its maximum population with respect to the other ions of the same element. These layers are listed in Table 2, column 1 shows the corresponding ions, column 2 gives the logarithm of the layer temperature (in K), column 3 the logarithm of $R_e = N_e T^{-3}$ (N_e is the electronic density in number). Each layer corresponds to the one about where the ion is supposed to give its maximum contribution to the total acceleration of the element. These same layers were used to obtain the results shown in Table 1.

The curves of Figs 4, 5 and 6 have to be compared with those shown in Fig. 1(b). In each figure we have pointed out the Lorentz limit, which is the value the derivative of individual g_{il} (equation 2) should reach in case of a pure Lorentz profile. We

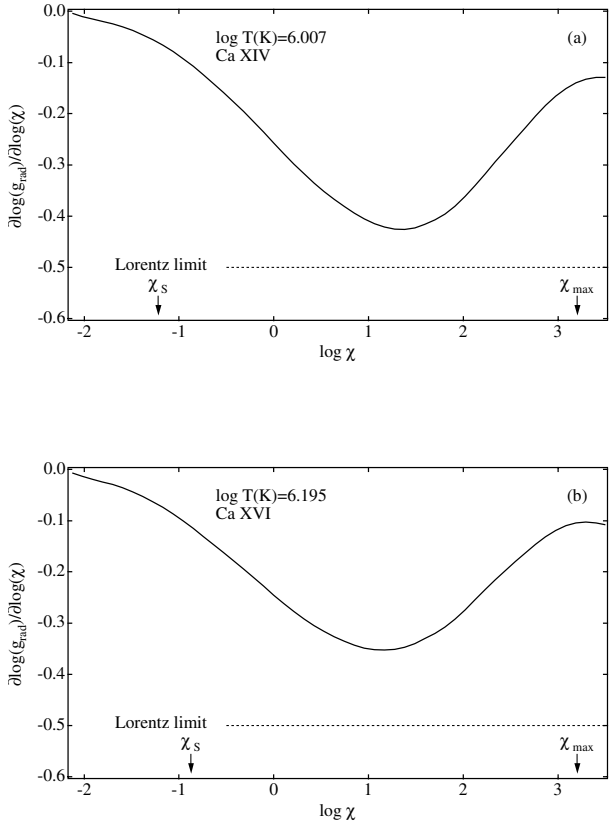

Figure 5. Same as Fig. 4 for (a) Ca XIV and (b) Ca XVI.

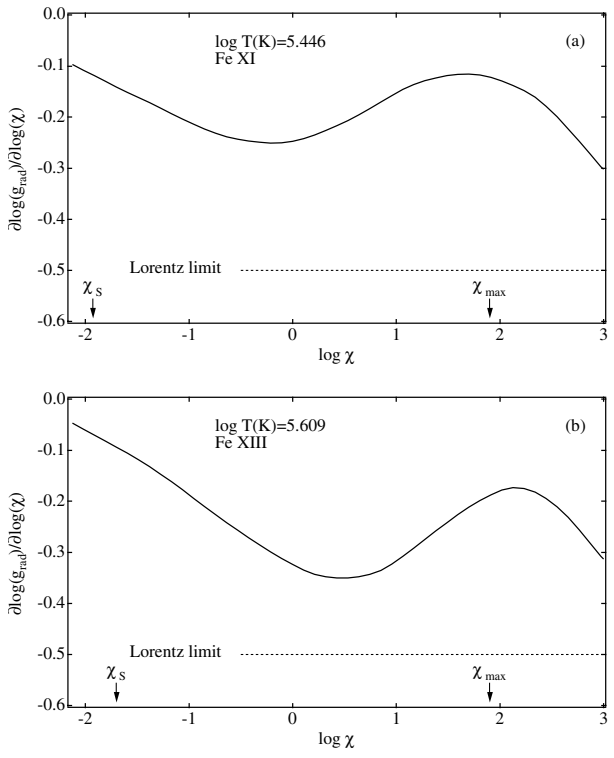

Figure 6. Same as Fig. 4 for (a) Fe XI and (b) Fe XIII.

Table 2. Layers where each ion has its maximum population with respect to the other ions of the same element.

Ion	log T	log R_e
Ar XIII	5.937	3.009
Ar XV	6.124	3.138
Ca XIV	6.007	3.069
Ca XVI	6.195	3.155
Fe XI	5.446	2.622
Fe XIII	5.609	2.723

have also shown, on the abundance axis (with two arrows), the values of log χ_S and log χ_{max} given in the two latter columns of Table 1. It should be noted that log χ_S corresponds to log $X=0$ in Fig. 1.

5 DISCUSSION

The results presented in Figs 4, 5 and 6 clearly show, for all the ions, that the three regions: 'unsaturated', 'saturated' and 'oversaturated' can be identified.

For all the considered ions, the 'unsaturated' regions appear rather small in the figures. This is owing to the low values of log χ_S and to the impossibility to carry out calculations for lower abundances from g_{rad} tables available at CDS, however, the trend toward constant accelerations exists.

The 'saturated' regions are well marked by a monotonic decrease of the derivatives, but the minimum never pass the Lorentz limit. This can be partly explained by the fact that accelerations from bound–free transitions are larger than the one assumed in Section 2. In that section, we had chosen arbitrarily $\gamma_{cont}=10^{-3}$, which corresponds to the assumption that the acceleration from bound–free transitions are 10^3 times smaller than the one owing to bound–bound transitions in the unsaturated case. This explanation is confirmed by the GLAM computations shown in Fig. 7 where we have plotted the ratio $g_{i,cont}/\Sigma_l g_{il}$ for the same ions and stellar layer as in Figs 4, 5 and 6. The GLAM results were used for this part of our study because the Seaton method does not permit the separation of accelerations owing to bound–bound and bound–free transitions. From these calculations one can suppose, at least for Ar and Ca ions for which a bending of the curves can be guessed for small log χ, that γ_{cont} is closer to 10^{-2} than to 10^{-3}. However, this explanation is not entirely satisfactory, since the minimum of Fe XI (Fig. 6a) is the farthest from the Lorentz limit whereas this ion has the smallest ratio $g_{i,cont}/\Sigma_l g_{il}$. Another factor could also contribute to this behaviour: the test particle approximation assumed in (4) probably does not apply to this ion, since Fe is an important source of opacity (see Fig. 8).

We have also considered the transition region between 'unsaturated' and 'saturated'. In this region the effect of γ_{cont} is still negligible, and then it can provide information about the dominant lines profile (Lorentz/Voigt/Gauss). We have computed the second derivatives of the accelerations and found that the acceleration have slopes close to, or less steep (with respect to the abundance) than the one owing to the Lorentz profile, i.e. α is around -0.5 or slightly larger.

The 'oversaturated' regions (where γ_{cont} is of the same order of magnitude than acceleration owing to lines) are also confirmed by Fig. 7 since the ratio $g_{i,cont}/\Sigma_l g_{il}$ are strongly increasing with the

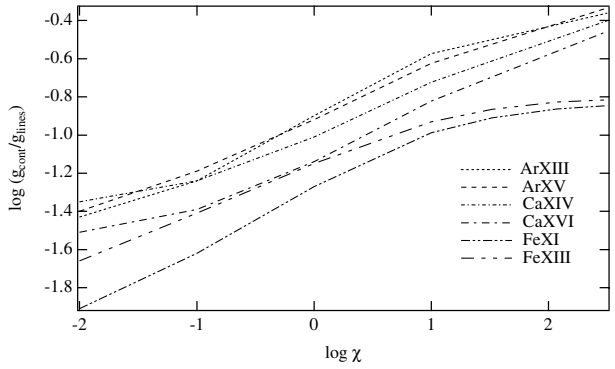

Figure 7. The ratio of the radiative acceleration owing to photoionization ($g_{\rm cont}$) to that of the lines ($g_{\rm lines}$) with respect to the abundance, for the various ions studied. Each curve is for a different layer corresponding to those listed in Table 2.

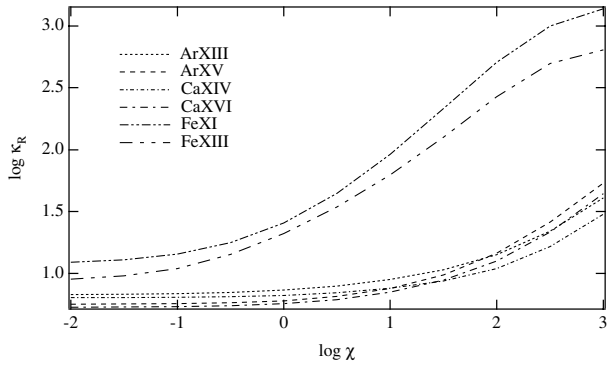

Figure 8. The Rosseland opacity log $\kappa_{\rm R}$ with respect to the abundance, for the various ions studied. Each curve is for a different layer corresponding to those listed in Table 2.

concentration and reach values larger than 0.1. For large χ, $g_{i,\rm cont}$ experience saturation effect, this is why bendings of the ratio appear in the far right part of the plot. A striking behaviour appears in Figs 5 and 6: the derivatives reach a maximum then decrease. This phenomenon is as a result of overmetallicity because it always occurs for abundances approximately larger than $\chi_{\rm max}$. This effect is not considered quantitatively significant, since the stellar model used here cannot be valid for such overabundances. It is clear that the schematic behaviours presented in Section 2 cannot apply here since the test particle approximation is certainly not satisfied. In that approximation, the average opacity in the medium is supposed to be independent of ion abundance. When an element becomes too overabundant, the average opacity in the medium is strongly affected by this element (see Fig. 8) and, certainly, new kind of behaviour must appear.

Line blending can also affect the accelerations for large abundances: the more a bound–bound transition is saturated, the larger the frequency interval, around the line centre, where its contribution to $g_{\rm rad}$ is significant. This implies that overlapping of lines should be important, at least for large abundances. We have tried to estimate this effect by comparing the accelerations when the monochromatic opacity $\kappa_{\rm tot\ b}$ is replaced by $\kappa_{\rm R}$ in equation (2). We have found (using the sampling method of LMR2000) that the ratio of the accelerations computed with $\kappa_{\rm tot\ b}$ over the ones computed with $\kappa_{\rm R}$, generally decrease with respect to the abundance. This could be interpreted as owing to the loss of line blending information when $\kappa_{\rm R}$ is used instead of $\kappa_{\rm tot\ b}$, however, we cannot draw firm conclusions in this work about that effect, since we cannot be sure that other unidentified effects are excluded.

6 CONCLUSIONS

In the present work, we have first formalized the classical knowledge about the behaviour of radiative accelerations according to the abundance of the element under consideration. To test this classical knowledge we have studied the logarithmic derivative of the acceleration (with respect to the abundance) for some typical ions which were selected among the few ones suitable for this purpose. The accelerations and the derivatives have been computed using accurate and detailed methods (GLAM, S97, LMR2000) in a typical main-sequence A-type star ($T_{\rm eff}$ = 10 000 K, log g = 4.31) where diffusion is able to produce large abundance anomalies. Our conclusions stand for metals not heavier than Iron, for which data are available for accurate computations, and stand for optically thick layers.

General behaviour of the accelerations appears compatible with the classical knowledge, however, our results point out some unexpected features. We have found that very few ions are unsaturated at a solar abundance, and that radiative accelerations tends partially toward a power law (with respect to the local concentration) in the transition region, between 'unsaturated' and 'saturated' cases. The power law with exponent α is not reached and this is owing to the following: (i) the photoionization component of acceleration is no more negligible when strongly saturated situation for lines is encountered (ii) the test particle approximation is not always valid (i.e. $\kappa_{\rm R}$ depends on the abundance of the ion considered). The exponent α has not been found to be smaller than -0.5 (pure Lorentz profile). This is not really surprising since collisional broadening dominates Doppler broadening in the considered stellar layers, but α appears larger than expected. We have also found that, in the 'oversaturated' case, saturation effects on photoionization and the effect of the variation of $\kappa_{\rm R}$ with respect to the abundance are noticeable.

ACKNOWLEDGMENTS

This research was partially funded by NSERC, and La Faculté des Études Supérieures et de la Recherche de l'Université de Moncton. We are indebted to M. J. Seaton for providing radiative accelerations of calcium in one of the stellar model used in this paper. We also thank J. Richer for providing some of the stellar models used for our calculations.

REFERENCES

Alecian G., 1985, A&A, 145, 275
Alecian G., 1994, A&A, 289, 885
Alecian G., Artru M.-C., 1990, A&A, 234, 323
Alecian G., Grappin R., 1984, A&A, 140, 159
Alecian G., Michaud G., 1981, ApJ., 245, 226
Alecian G., Michaud G., Tully J., 1993, Apj, 411, 882
Alecian G., Vauclair S., 1983, Fundam. Cosmic Phy., 8, 369
Cunto W., Mendoza C., Ochsenbein F., Zeippen C., 1993, A&A, 275, L5
Gonzalez J.-F., Artru M.-C., Michaud G., 1995a, A&A, 302, 788
Gonzalez J.-F., LeBlanc F., Artru M.-C., Michaud G., 1995b, A&A, 297, 223 (GLAM)
Kurucz R. L., 1990, in McNally D., ed., Trans. IAU Vol. XXB. Kluwer, Dordrecht, p. 168

Kurucz R. L., 1991, in Crivelari L., Hubeny I., Hummer D. G., eds, Stellar Atmospheres: Beyond Classical Models. Kluwer, Dordrecht, p. 441
LeBlanc F., Michaud G., 1995, A&A, 303, 166
LeBlanc F., Michaud G., Richer J., 2000, ApJ, 538, 876 (LMR2000)
Legris G., 1998, Utilisation du code de M. J. Seaton dans l'étude des accélérations radiatives dans les enveloppes d'étoiles', stage de DEA
Massacrier G., 1996, A&A, 309, 979
Michaud G., 1970, ApJ, 160, 641
Michaud G., Charland Y., Vauclair S., Vauclair G., 1976, ApJ, 210, 447
Richer J., Michaud G., 1993, Apj, 416, 312
Richer J., Michaud G., Rogers F., Iglesias C., Turcotte S., LeBlanc F., 1998, ApJ, 492, 833
Richer J., Michaud G., Turcotte S., 2000, ApJ, 529, 338
Rogers F. J., Iglesias C. A., 1992a, ApJS, 79, 507
Rogers F. J., Iglesias C. A., 1992b, Apj, 401, 361
Seaton M. J., 1997, MNRAS, 289, 700 (S97)
Seaton M. J., Zeippen C. J., Tully J. A., Pradhan A. K., Mendoza C., Hibbert A., Berrington K. A., 1992, Rev. Mex. Astron. Astrofis., 23, 19
Turcotte S., Richer J., Michaud G., 1998a ApJ, 504, 559
Turcotte S., Richer J., Michaud G., Iglesias C. A., Rogers F. J., 1998b ApJ, 504, 539

This paper has been typeset from a Microsoft Word file prepared by the author.